

Finite temperature pion vector form factors in Chiral Perturbation Theory

A. Gómez Nicola, F. J. Llanes-Estrada and J. R. Peláez.

Departamentos de Física Teórica I y II. Univ. Complutense. 28040 Madrid. SPAIN.

Abstract

We discuss the thermal structure of the vector pion form factors and calculate them in one-loop Chiral Perturbation Theory. The perturbative result is used to analyze the T -dependent electromagnetic pion charge radius, obtaining an estimate of the deconfinement critical temperature. In addition, imposing thermal unitarity, we generate the resonance in the center of mass form factor, whose peak, mass and width thermal variations are compatible with those observed in dilepton production in Relativistic Heavy Ion Collisions.

PACS: 11.10.Wx, 12.39.Fe, 11.30.Rd, 25.75.-q., 12.38.Mh.

1 Introduction

Ongoing experiments on Relativistic Heavy Ion Collisions (RHIC) have attracted much attention over the past years. After the expected Quark-Gluon-Plasma cools down and hadronic matter forms, a correct description of the system involves QCD at temperatures below the chiral phase transition. In this regime, the medium constituents are predominantly light mesons, whose very low-energy dynamics is described by Chiral Perturbation Theory (ChPT) [1, 2], the low-energy effective theory of QCD based on spontaneous chiral symmetry breaking. ChPT is a low-energy expansion performed in terms of $p^2 = -\vec{p}^2$ with p a typical meson energy or temperature and $T \sim 1 \text{ GeV}$. It has been successfully applied to light meson dynamics and also to describe the low- T pion gas [3]. Recently, we have calculated in this framework the thermal scattering amplitude [4] and its unitarization [5] showing that chiral symmetry and unitarity alone provide a reasonable description of the thermal and resonances, without including them as explicit degrees of freedom (see also [6]).

One salient observable in RHIC is the dilepton spectrum: $e^+ e^-$ pairs are direct probes of the plasma evolution, since they do not interact from the production point to the detector. The observed spectrum for invariant masses between 200 MeV and 1 GeV differs significantly from vacuum hadronic emission models and calibrating collisions with light

ions, showing a global enhancement [7] for which different explanations have been proposed [8, 9, 10]. This effect is particularly visible near the mass, around which the spectrum attens and is compatible with a widening of the [8, 10, 11] as we indeed obtained in [4, 5]. Ignoring baryon density effects, a reasonable approximation for central rapidity, the main contribution to the dilepton spectrum at low energy stems from the annihilation of two thermal pions via the emission of a virtual photon $e^+ e^- \rightarrow \gamma \rightarrow e^+ e^-$ [12, 13, 8, 10] where the γ is produced as an intermediate resonant state. Thus, the production rate for dileptons is governed by the pion form factor [12, 13] whose modification in the pion gas is key to the spectrum [8, 10, 14]. Prior calculations have relied on model dependent input, the closest to our approach being the finite temperature form factor analysis in [14], a chiral model with resonances explicitly included as independent fields. In this work we first present a model independent study of the finite temperature effects on the pion form factor using ChPT. In particular, after a brief analysis of the different thermal form factors in Section 2, we obtain the one-loop ChPT thermal calculation, we study the temperature evolution of the pion electromagnetic charge and radius, obtaining a rough estimate of the critical temperature of deconfinement, and we check thermal unitarity. Later on, in Section 4, we implement unitarity to describe the effect of the thermal variation of the resonance mass and width in the form factor. In section 5 we summarize our main results.

2 Finite temperature vector form factors

At $T \neq 0$, all physical quantities may depend on the uid four-velocity, so that, with the usual choice of the uid rest frame, Lorentz covariance is lost while spatial rotation covariance is still preserved. Therefore, the most general expression for the timelike vector form factor of charged pions, or electromagnetic $e^+ e^-$ vertex, is:

$$\begin{aligned} h^+(p) \cdot (p^0) \mathcal{V}_0(0) \not{p}_i &= q_b F_t(S_0; \not{p} \not{q}_b) \\ h^+(p) \cdot (p^0) \mathcal{V}_k(0) \not{p}_i &= q_k F_s(S_0; \not{p} \not{q}_b) + S_k q_b G_s(S_0; \not{p} \not{q}_b) \end{aligned} \quad (1)$$

with \mathcal{V} the electromagnetic current, $S = p + p^0$, $q = p - p^0$ and F_t, F_s, G_s even functions in q_b (charge conjugation invariance). Note that the effect of Lorentz covariance breaking is twofold: on the one hand, the time and spatial components of the current may depend on the three different functions F_t, F_s and G_s and, on the other hand, those functions may

depend on three independent rotationally invariant variables, instead of just one invariant variable ($s = S^2$) as in the $T = 0$ case. Terms containing $\epsilon_{ijk} S^i q^j$, allowed by rotation invariance and C are forbidden by parity.

Of course, gauge invariance further restricts the above expressions, imposing relations between the functions $F_{t,s}; G$. When taking the divergence of the current, it must be also taken into account that the in-medium pion dispersion relation may be different from the vacuum one, i.e., the pole of the pion propagator is at $p^2 = m^2 + g(p_0; p; T)$ with g a complex function. Altogether, this relates the form factors and the function g . However, we will content ourselves here with one-loop ChPT, which gives the real (and positive) leading $O(p^4)$ to g , that depends on T but not on energy and momentum [3]. That is, to $O(p^4)$ the two pions in (1) can be treated as free with a T -dependent mass shift. Therefore, to $O(p^4)$ we have $q \cdot S = 0$ that combined with gauge invariance $\partial^\mu V \partial_\mu = 0$ in (1) yields:

$$S_0 F_t^{(1)} F_s^{(1)} = \mathcal{F}_t^2 G_s^{(1)} \quad (2)$$

where the superscript (1) means the NLO (one-loop) form factors. Remember that the (T -independent) leading order is just $F_t^{(0)} = F_s^{(0)} = 1, G_s^{(0)} = 0$.

As we will see below, in one-loop ChPT $G_s^{(1)} \neq 0$ and therefore there are two independent thermal form factors $F_t^{(1)} \neq F_s^{(1)}$. Moreover, there is an additional simplification valid to one loop: the $F_t; F_s; G_s$ functions do not depend on q_0 . Our previous gauge invariance condition (2) coincides with the analysis performed in [14].

3 One loop ChPT calculation

In this section we follow similar steps as in our pion scattering calculation [4]. We calculate the time-ordered product of two pion and one current fields in the imaginary time formalism (ITF) of Thermal Field Theory [15]. This we continue analytically for continuous external pion energies and connect to the form factor through the LSZ reduction formula. Such thermal amplitudes correspond to retarded real-time Green functions and have the correct analytic and unitarity structure [4, 5], properties of special interest in this study.

In the ITF, the lagrangian and electromagnetic current coincide with those in ordinary $T = 0$ ChPT. The thermal corrections arise upon replacing all zeroth momentum com-

ponents by discrete frequencies k^0 ! $i!_n = 2$ inT and the loop integrals by M atsubara sum s, i.e., $\frac{R}{2} \frac{dk^0}{2} ! iT \sum_{n=1}^P$. We draw in Figure 1 the diagrams (also the same as for $T = 0$) contributing to the form factors at NLO within the SU(2) chiral lagrangian [2].

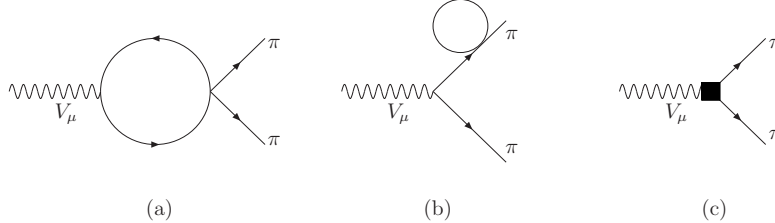


Figure 1: Diagrams contributing to the pion form factors to one loop in ChPT.

Diagram (a) gives, among other contributions, the imaginary part needed for unitarity (see section 3.2) while diagram (b) is proportional to the T -dependent tadpole which is real and affects the electromagnetic vertex through wavefunction renormalization. Their iTF contributions to the current expectation value, before performing the analytic continuation are given by:

$$\begin{aligned}
 h^+ \mathcal{J} \mathcal{V} \mathcal{D} i_{(a)} &= \frac{2q}{f^2} T \sum_{n=1}^{n \bar{X}+1} Z \frac{d^{D-1} k}{(2)^{D-1}} \frac{k \cdot k}{(k^2 - m^2)((k - S)^2 - m^2)} \\
 h^+ \mathcal{J} \mathcal{V} \mathcal{D} i_{(b)} &= \frac{q}{f^2} T \sum_{n=1}^{n \bar{X}+1} Z \frac{d^{D-1} k}{(2)^{D-1}} \frac{1}{k^2 - m^2}
 \end{aligned} \tag{3}$$

where $S_0; k_0$ 2 iT Z and D is the space-time dimension. As for diagram (c), the black box stands for the $O(p^4)$ lagrangian tree level contribution, and therefore T -independent, proportional to the low-energy constant l_6 [2].

The integrals appearing in (3) can be related to the T -dependent one-loop integrals discussed in the Appendix of [4]. We adhere to the notation and conventions of that work. Using the formulae there quoted and after analytic continuation, the form factors can be written in terms of three independent thermal integrals: $J_2; J_0$, that are energy and momentum dependent, and the constant tadpole integral F^{-1} :

$$\begin{aligned}
 F_t^{(1)}(S_0; \mathcal{S}) &= \frac{s}{2f^2 \mathcal{S}^2} \frac{h}{4} J_2(S_0; \mathcal{S}) - S_0^2 J_0(S_0; \mathcal{S}) - 2 F^{-1} \\
 F_s^{(1)}(S_0; \mathcal{S}) &= \frac{1}{4f^2} \frac{s}{\mathcal{S}^2} \frac{h}{4} J_2(S_0; \mathcal{S}) - S_0^2 J_0(S_0; \mathcal{S}) - 2 F^{-1}
 \end{aligned}$$

¹We have used $J_1(S_0; \mathcal{S}) = \frac{S_0}{2} J_0(S_0; \mathcal{S})$, that holds for any $S_0; \mathcal{S}$.

$$\begin{aligned}
& + (4m^2 s) J_0(S_0; \mathfrak{F}) \underset{\substack{i \\ \text{---}}}{} 4 F \\
G_s^{(1)}(S_0; \mathfrak{F}) & = \frac{S_0}{4f^2 \mathfrak{F}^2} \frac{3s}{\mathfrak{F}^2} \underset{\substack{i \\ \text{---}}}{} 4 J_2(S_0; \mathfrak{F}) \underset{\substack{i \\ \text{---}}}{} S_0^2 J_0(S_0; \mathfrak{F}) \underset{\substack{i \\ \text{---}}}{} 2 F \\
& + (4m^2 s) J_0(S_0; \mathfrak{F}) \underset{\substack{i \\ \text{---}}}{} 4 F
\end{aligned} \tag{4}$$

As in [4], for a T -dependent quantity we denote $H(T) = H(T) - H(0)$. Recall that all the $D = 4$ UV divergences are contained in the $T = 0$ part [2] that is finite and scale independent once expressed in terms of the finite and scale independent constant l_6 and the subtracted $T = 0$ loop integral $J(s) = J_0(s) - J_0(0)$

$$F_T(s) = F_s(s) = 1 + J(s) \frac{s}{6f^2} \frac{4m^2}{(l_6 - 1/3)s} : \tag{5}$$

We remark that our finite temperature additions (4) are written in Minkowski space-time for continuous $S_0 \in \mathbb{R}$. In addition, we have used the on-shell condition $p^2 = (p^0)^2$, valid to one loop. As we mentioned in section 2, the one-loop form factors do not depend on q_0 . For instance, there are terms in H_0 proportional to $q_0 S = q_0 S_0$ to this order that would otherwise give a nontrivial q_0 dependence. Finally, note that in the above expression and to this order we can use either the physical f, m , their tree level values or their T -dependent ones, since the differences are of higher order. We have chosen to write down our expressions in terms of the $T = 0$ physical values $f = 92.4$ MeV, $m = 139.6$ MeV.

It is easy to check the consistency of our explicit one-loop form factors (4) with the gauge identity (2), showing how $G_s^{(1)} \neq 0$ for arbitrary $S_0; \mathfrak{F}$. Another interesting check concerning the unitarity of (4) in the center of mass frame will be analyzed in section 3.2.

3.1 Pion electromagnetic charge and radius at $T \neq 0$.

A direct prediction of our ChPT calculation is the pion electromagnetic static charge density at $T \neq 0$ and low energies. Recall that at $T = 0$, the total pion charge and charge radius are $hQ i_0 = F(0)$ and $hr^2 i_0 = 6F'(0) = F(0)$ where $F(s)$ is the form factor. Thus, from (5), $hQ i_0 = 1$ and $hr^2 i_0 = (l_6 - 1) = 16^{-2}f^2$. In fact, this is the simplest way to fix the value of l_6 in ChPT. With the experimental value $hr^2 i_0 = 0.45 - 0.01$ fm² [16] one gets $l_6 = 16.6 - 1.4$.

Likewise, at $T \neq 0$ taking into account the Lorentz covariance breaking:

$$hr^2 i_T = \frac{6}{Q_T} \frac{dF_t(0; \vec{p})}{d\vec{p}^2} \Big|_{\vec{p} \neq 0} \quad (6)$$

where $Q_T = \lim_{\vec{p} \neq 0^+} F_t(0; \vec{p}; T)$. Note that the charge density is defined through V_0 and hence F_t in (1) must be used. We consider the spacelike radius as would be measured in t-channel e scattering and therefore S_0 must be set to zero before \vec{p} (static limit). Analogous timelike and magnetic moment radii could also be defined. From equation (4) we find:

$$\begin{aligned} Q_T &= 1 - \frac{1}{2^2 f^2} \int_m^{\infty} dE \frac{2E^2 - m^2}{E^2 - m^2} n_B(E; T) \\ Q_T hr^2 i_T &= hr^2 i_0 + \frac{1}{12^2 f^2} \int_m^{\infty} dE \frac{3(E^2 - m^2)(E^2 + 2m^2)}{E^4 - m^2} n_B(E; T) \\ &\quad + \frac{E(2E^4 + 2m^4 - E^2 m^2)}{E^2 m^2} \frac{dn_B(E; T)}{dE} \end{aligned} \quad (7)$$

where $n_B(x; T) = [\exp(x/T) - 1]^{-1}$ is the Bose-Einstein distribution function.

Note that the charge decreases with temperature due to $O(T^2)$ corrections in the static limit. This is similar to the electric charge Debye screening in QED [15, 17]. For the negatively charged pion, the whole eq. (7) changes sign, thus increasing with T , so that the gas remains neutral. We have plotted $hr^2 i_T = hr^2 i_0$ in Figure 2. The T -correction is almost negligible below 100 MeV, where it decreases very slightly. For higher T , the radius increases considerably, the dominant contribution coming from the Q_T screening discussed above. Since they rely on ChPT alone, these results are model independent.

We get a rough estimate of the deconfinement temperature T_c [17] when the pion electromagnetic volume equals the inverse pion density, i.e., $(4\pi^2)hr^2 i_T^{3/2} = 1 = n(T)$, where $n(T) = 3 \frac{d^3 \vec{p}}{(2\pi)^3} n_B(-\vec{p}; T)$. Taking just $hr^2 i_0$ gives $T_c \approx 265$ MeV, which is clearly too high, as commented in [17]. Thus, the thermal increase of $hr^2 i_T$ reduces T_c to a more realistic value and in fact, with our above result we get $T_c \approx 200$ MeV. The uncertainties in λ amount to ≈ 4 MeV. This critical temperature is below the temperature where $Q_T = 0$ and the radius diverges, which would correspond to a vanishing pion thermal mass and is clearly beyond the validity range of the chiral expansion. As a matter of fact, these estimates have to be regarded as merely qualitative.

Also, the pion form factor can be approximated at low energy by a monopole form with a pole corresponding to the ρ , allowing the estimate $\lambda / f^2 \approx M^2$ in the VMD limit

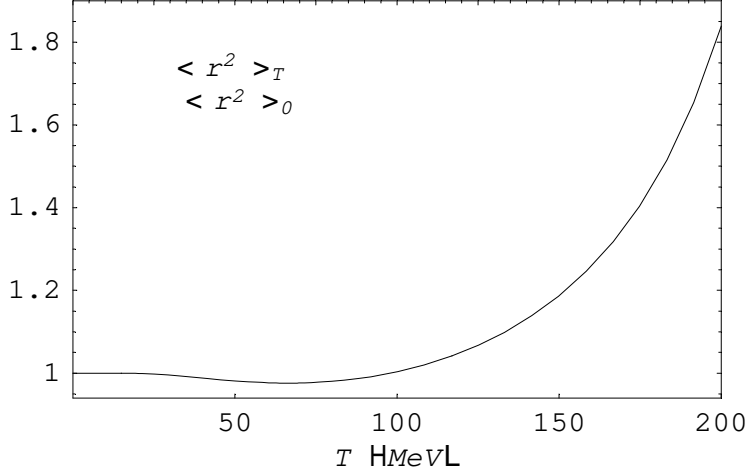


Figure 2: The electromagnetic pion charge radius at $T \neq 0$.

[18]. Therefore, the electromagnetic radius is proportional to M^{-2} . Thus, at $T \neq 0$, our previous results, still model-independent, would suggest an almost constant (though slightly increasing) $M(T)$ for very low T and a clearly decreasing $M(T)$ for $T > 100$ MeV. This is indeed the behaviour that we found in [5] and is also confirmed by our analysis in section 4. Such behaviour for $M(T)$ at very low T is a prediction of chiral symmetry and resonance saturation, at least in the chiral limit [19].

3.2 Thermal perturbative unitarity in the center of mass frame

Let us reduce our previous expressions to the center of mass frame (c.m.), i.e., $p = \hat{p}^0$ in (1). This amounts to look only to back to back $e^+ e^-$ pairs in the dilepton spectrum. The dilepton rate is particularly simple in that case [13] although the angular dependence may be important when performing more realistic analysis [10].

Therefore, we take the limit $\not{p} \rightarrow 0^+$ in our previous expressions. Noting that $J_2 = (S_0^2 - 4)J_0 + F = 2 + O(\not{p})$ [4] we see in (4) that $F_t^{(1)}$, $F_s^{(1)}$ and $\not{p}^2 G_s^{(1)}$ have a finite c.m. limit, which is reassuring. In addition, in the c.m. frame $(p - p^0)(p + p^0) = 0$ implies $S_k q_k G_s = S_k (2S^j p^j - S_0)G_s = 2p_k (\not{p}^2 G_s - S_0) = q_k (\not{p}^2 G_s - S_0)$ so that $\not{p}^2 G_s = S_0$ can be reabsorbed in F_s in (1). Finally, we find:

$$\begin{aligned} \lim_{\not{p} \rightarrow 0^+} F_t^{(1)}(S_0; \not{p}) &= \lim_{\not{p} \rightarrow 0^+} F_s^{(1)}(S_0; \not{p}) = \frac{1}{6f^2} \frac{h}{S_0^2 - 4m^2} J_0(S_0; 0) + 4 F \\ \lim_{\not{p} \rightarrow 0^+} \not{p}^2 G_s^{(1)}(S_0; \not{p}) &= 0 \end{aligned} \quad (8)$$

Therefore, in the c.m. frame there is only one T -dependent form factor, which we

will just call $F(S_0; T)$ for simplicity. The tadpole contribution F is real, while J_0 contains a nonzero imaginary part required by unitarity. In fact, following the same steps as in [4]:

$$\text{Im } F^{(1)}(E + i\epsilon; T) = \text{Tr}(E) \frac{E^2 - 4m^2}{96 f^2} \quad (9)$$

with

$$\text{Tr}(E) = (E^2) [1 + 2n_B(E=2; T)] \quad (10)$$

for positive energies above the two-pion threshold $E > 2m$. Here, $\text{Tr}(s) = \frac{P}{1 - 4m^2/s}$ is the two-pion phase space factor.

At $T = 0$, (9) is the perturbative version of the form factor unitarity relation $\text{Im } F(s) = (s)F(s)a^{11}(s)$ where a^{11} is the $I = J = 1$ partial wave projection of the scattering amplitude (to lowest order $F = 1$ and $a^{11}(s) = (s - 4m^2)/96 f^2$). At $T \neq 0$, the correction factor $1 + 2n_B = (1 + n_B)(1 + n_B) - n_B n_B$ is interpreted as enhanced phase space [20] due to the difference between induced emission and absorption processes [4]. Therefore, we find that the form factor satisfies a perturbative unitarity relation analogous to that in the $T = 0$ case, but now in terms of a thermal phase space factor. The same happened with the thermal amplitude in [4]. This is not only a consistency check of our calculation, but it will be the basis of our unitarization method used in the next section in order to generate the pole in the form factor.

4 Unitarization and applications

The ChPT perturbative form factors analyzed in the previous sections provide the prediction of chiral symmetry to next to leading order and at finite temperature. However, by construction, they cannot reproduce a pole or resonant behaviour, which in the $I = J = 1$ channel corresponds to the $\pi\pi$ scattering amplitude. Our approach here will be to construct a nonperturbative thermal form factor F imposing exact thermal unitarity with respect to the nonperturbative pion scattering amplitude. The latter is well approximated by the Inverse Amplitude Method (IAM) [21] derived at $T \neq 0$ in [5] $a^{\text{IAM}}(E; T) = a_1^2(E^2) = [a_1(E^2) - a_2(E; T)]$ where a_1 and a_2 are the ChPT partial waves to tree and one-loop level respectively (we are suppressing the 11 superscript). The IAM amplitude is also exactly unitary, ie, $\text{Im } a^{\text{IAM}} = \text{Tr} a^{\text{IAM}} \neq 0$ so that our only physical input, apart from chiral symmetry, will be unitarity. It should be borne in mind that our approach of demanding exact thermal elastic unitarity is meant to be valid for energies and temperatures such that $n_B(E=2; T) \ll 1$.

remains small [5]. For the dilepton spectrum this means that for typical freeze-out temperatures $T \gtrsim 150$ MeV, our approach is rather accurate around the scale, which is precisely where unitarity is saturated. Near the pion pair threshold, corrections to pion propagation not included in this work (nominally of $O(p^6)$ in ChPT) have been conjectured to be more important [13, 14, 10].

If we take F / a^{IAM} with a real proportionality constant we readily guarantee the exact unitarity condition $\text{Im } F = {}_T F a^{\text{IAM}}$ and also that both the amplitude and the form factor have the same poles in the complex plane as well as the same complex phase (phase shift), as it happens for $T = 0$. Imposing the correct low energy perturbative ChPT expansion $F = 1 + F^{(1)} + \dots$ the real proportionality constant is fixed as follows:

$$F(E; T) = \frac{1 + \text{Re} F^{(1)}(E; T)}{a_2(E^2) + \text{Re} a_4(E; T)} \frac{a_2^2(E^2)}{a_2(E^2) - a_4(E; T)}; \quad (11)$$

valid for $E > 2m$, where perturbative unitarity holds. The above formula was developed at $T = 0$ in the strongly interacting electroweak spontaneous symmetry breaking sector [22]. At low energies it reproduces the chiral expansion up to $F^{(1)}$ plus terms of higher order, which should be smaller. Thus we expect that it should reproduce also the low energy data with an l_6 value slightly different, but reasonably close, to that used in the previous section with the pure one-loop ChPT. All that remains is to adjust the undetermined low-energy constant l_6 to zero-temperature experimental data and the finite T behavior follows as a prediction. For a^{IAM} we use the very same calculation given in [5]. In Figure 3a we show how the data [23] are nicely described by the resulting phase shift in the 11 channel, common to the amplitude and the form factor. This fixes the form factor phase. In Figure 3b, we plot $|F(E; 0)|^2$ for 0.3 GeV $< E < 1$ GeV compared with the data in [24]. The solid line has been obtained with $l_6 = 18$, which describes data reasonably well and is compatible with the perturbative value quoted in section 3.1. For illustration we also provide curves with $l_6 = 17$ (dotted) and $l_6 = 19$ (dashed). Observe that the resonant behaviour around $M \approx 770$ MeV is clearly reproduced in both figures. In fact, note that the unitarized formula gives exactly the form factor phase and therefore the position and width of the pole is very accurately reproduced. However, the modulus is more subject to perturbative uncertainties, as reflected in Figure 3.

Next, in Figure 4 we have plotted $|F(E; T)|^2$ for different temperatures. We observe that the form factor decreases and widens with temperature. The mass position of the peak moves slightly to the right at first and then lowers in the $T = 150$ MeV curve,

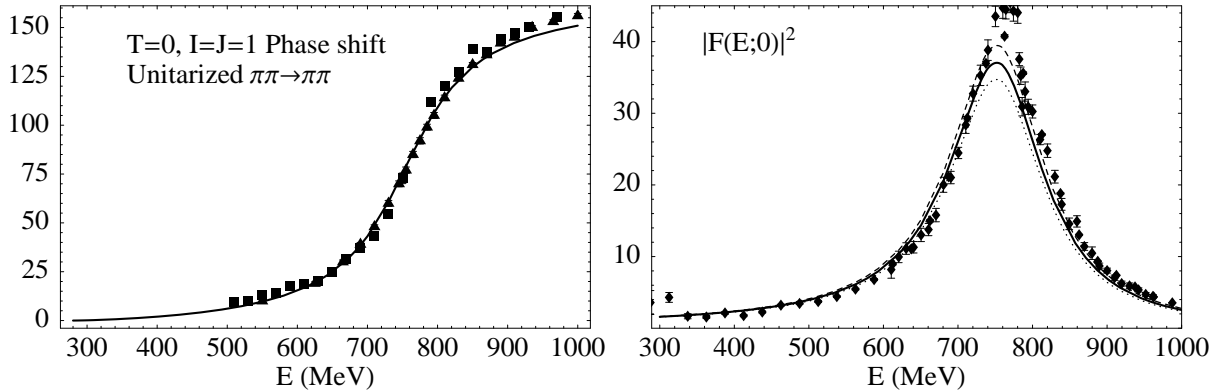


Figure 3: a) We show the phase of the a^{IAM} for elastic amplitude of scattering in the rho channel. The data comes from [23] b) The unitarized form factor at temperatures $T = 0$, for $l_6 = 18$ (solid line), $l_6 = 17$ (dotted line) and $l_6 = 19$ (dashed line). The data comes from [24].

consistently with our discussion on the pion electromagnetic radius in section 3.1. Note that, by construction, the form factor (11) has a peak exactly at the same place and with the same width as the amplitude, that we had already studied in [5], and where the pole moved further away from the axis, explaining the strong attening of the form factor in this work.

Our results agree with [14]. Note however that we have not introduced explicit resonances, the physical assumptions are just chiral symmetry and unitarity. Our $T = 0$ peak also falls a little bit short of the data but much closer than [14]. Since we only deal with two pions, and therefore only the resonance, this could be partially due to π^0 contamination in the data coming from e^+e^- annihilation (rst reference in [24]). Indeed, the lowest data point at the peak, closer to our curves, comes from decay (second reference in [24]), where no π^0 can be produced. The two-loop calculation [25] can also improve the situation, but this is beyond our scope at $T \neq 0$.

Our unitarized form factor is also fully consistent with expectations from the dilepton spectrum data. The form factor enters directly in the dilepton rate from pion annihilation [12, 13]. In fact, in the com. and in thermal equilibrium the rate is proportional to $n_B^2(E=2;T)F(E;T)^2$ [13]. When the primary meson decay contribution is added but taking $F(E;0)$, the theoretical prediction exceeds the dilepton data around $M = 100$ GeV. Therefore medium effects need to reduce the form factor. Moreover the form factor is expected to spread by a factor of two at $T = 150$ MeV [10] simultaneously decreasing the peak position. These effects are visible in our theoretical result for the form factor,

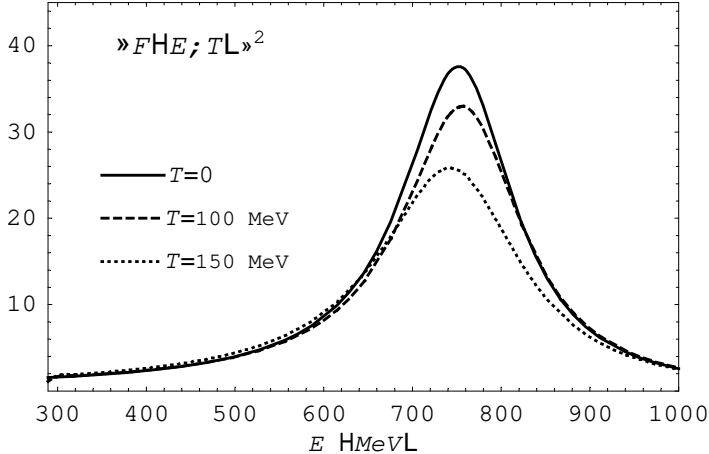


Figure 4: The unitarized form factor at temperatures $T = 0, 100, 150$ MeV.

while we estimate the peak mass position decrease to be somewhat smaller than assumed for instance in [10]. However, it is worth pointing out that a recent measurement by the STAR collaboration at RHIC [26] of the π^0 in-medium properties directly in $\pi^0 \pi^+ \pi^-$ shows a softer mass decrease (of about -40 MeV) and therefore much closer to the size of our predictions. This is an important measurement, as chiral symmetry restoration requires that π^0 and a_1 become degenerate [27] so that this predicts a sharp a_1 mass decrease. Further lowering of the mass as measured in pion observables can be achieved theoretically due to various in-medium effects [28] such as collisional broadening, the Boltzmann factor and rescattering at later stages of the collision (lower temperatures).

5 Conclusions

We have analyzed the pion form factors at finite temperature in Chiral Perturbation Theory. The general structure of the form factors at $T \neq 0$ allows in principle for three different form factors. However, the gauge Ward-Takahashi identity constrains them, relating the form factors to the in-medium pion dispersion relation.

Our explicit one-loop calculation gives the two different form factors not tied by gauge invariance with the correct $T = 0$ limit. In the center of mass frame, the two form factors coincide and satisfy a perturbative thermal unitarity relation in terms of a thermal phase space, consistently with our previous results on the thermal scattering amplitude. Using only ChPT, we have studied how the effective charge and charge radius of the pion

change with temperature. The effective charge is screened with T , while the radius is almost constant for low T and then increases, consistently with the mass behaviour and with estimates of the deconfinement temperature.

Demanding exact thermal unitarity and compliance with Chiral perturbation Theory at low energies allows to construct a nonperturbative thermal form factor which reproduces previous theoretical analysis and whose behaviour is compatible with the observed dilepton spectrum. At the typical freeze-out temperatures of $T' \approx 150$ MeV, our result predicts a bulk decrease and spreading of the form factor curve in the relevant range of energies around the scale, as expected from dilepton data. In addition, the position of the peak is slightly moved to the left. We have arrived to our result imposing only chiral symmetry and thermal unitarity as physical assumptions.

The unitarization method discussed here is limited to the center of mass frame. For future work, it would be interesting to extend these ideas including the angular dependence needed for the dilepton analysis. According to our discussion above, this would need to account simultaneously for the effect of different form factors and the dispersion relation. Still, an analysis of back-to-back lepton data by ongoing experimental collaborations would allow comparison with these very simple and powerful theoretical results. In addition, a more realistic study should also include the space-time evolution of the plasma and baryon density effects. Work is in progress along these directions.

Acknowledgments

Work supported from the Spanish CICYT projects, FPA 2000-0956, PB 98-0782 and BFM 2000-1326.

References

- [1] S. Weinberg, *Physica* A 96, 327 (1979).
- [2] J. Gasser and H. Leutwyler, *Annals Phys.* 158, 142 (1984).
- [3] J. Gasser and H. Leutwyler, *Phys. Lett. B* 184, 83 (1987).
- [4] A. Gómez Nicola, F. J. Llanes-Estrada and J. R. Peláez, *Phys. Lett. B* 550, 55 (2002).
- [5] A. Dobado, A. Gómez Nicola, F. Llanes-Estrada and J. R. Peláez, *Phys. Rev. C* 66, 055201 (2002).
- [6] A. Gómez Nicola, J. R. Peláez, A. Dobado and F. J. Llanes-Estrada, *AIPE Conf. Proc.* 660 (2003) 156 [[arXiv:hep-ph/0212121](https://arxiv.org/abs/hep-ph/0212121)].

[7] P.A. Seidt et al [DLS Collaboration], *Nucl. Phys. A* 525 (1991), 299c. M. Asena et al [HELIOS/3 Collaboration], *Nucl. Phys. A* 590 (1995), 93c; G. A. Gakidiev et al [CERES Collaboration] *Phys. Rev. Lett.* 75 (1995), 1272; *Phys. Lett. B* 442, 405 (1998); *Nucl. Phys. A* 661, 23 (1999); D. Adamova et al [CERES/NA45 Collaboration], *Phys. Rev. Lett.* 91, 042301 (2003).

[8] G. Q. Li, C. M. Ko and G. E. Brown, *Phys. Rev. Lett.* 75, 4007 (1995).

[9] V. Koch and C. Song, *Phys. Rev. C* 54 (1996), 1903. R. Rapp, J. Wambach, *Adv. Nucl. Phys.* 25:1 (2000); A. Ayala, [arxiv:hep-ph/0305170](https://arxiv.org/abs/hep-ph/0305170). T. Renk and A. M. Ishra, [arxiv:nucl-th/0312039](https://arxiv.org/abs/nucl-th/0312039).

[10] H. J. Schulze and D. Blaschke, *Phys. Lett. B* 386, 429-436 (1996); *Part. Nucl. Lett.* 119, 27 (2004).

[11] V. L. Eletsky, M. Belkacem, P. J. Ellis and J. I. Kapusta, *Phys. Rev. C* 64, 035202 (2001).

[12] K. Kaantie, J. Kapusta, L. McLerran, A. Mekjian, *Phys. Rev. D* 34, 2746 (1986).

[13] C. Gale and J. Kapusta, *Phys. Rev. C* 35, 2107 (1987); *C* 38, 2659 (1988).

[14] C. Song and V. Koch, *Phys. Rev. C* 54, 3218 (1996).

[15] M. Le Bellac, *Thermal Field Theory* (Cambridge University Press, 1996).

[16] Review of Particle Physics. K. Hagiwara et al., *Phys. Rev. D* 66, 010001 (2002).

[17] J. I. Kapusta, *Finite-temperature field theory* (Cambridge University Press, 1989).

[18] J. F. Donoghue, C. Ramirez and G. Valencia, *Phys. Rev. D* 39, 1947 (1989); G. Ecker, J. Gasser, A. Pich and E. de Rafael, *Nucl. Phys. B* 321, 311 (1989).

[19] M. Dey, V. L. Eletsky and B. L. Ioane, *Phys. Lett. B* 252, 620 (1990).

[20] H. A. Weldon, *Ann. Phys.* 214 (1992), 152.

[21] T. N. Truong, *Phys. Rev. Lett.* 61, 2526 (1988); *Phys. Rev. Lett.* 67, 2260 (1991); A. Dobado, M. J. Herrero and T. N. Truong, *Phys. Lett. B* 235, 134 (1990); A. Dobado and J. R. Pelaez, *Phys. Rev. D* 47, 4883 (1993); *Phys. Rev. D* 56, 3057 (1997).

[22] A. Dobado, M. J. Herrero, J. R. Pelaez and E. Ruiz Morales, *Phys. Rev. D* 62, 055011 (2000).

[23] S. D. Protopopescu et al., *Phys. Rev. D* 7 (1973) 1279. P. Estabrooks and A. D. Martin, *Nucl. Phys. B* 79, 301 (1974).

[24] R. R. Akhmetshin et al. [CMD-2 Collaboration], *Phys. Lett. B* 578, 285 (2004) S. Anderson et al. [CLEO Collaboration], *Phys. Rev. D* 61, 112002 (2000).

[25] T. Hannah, *Phys. Rev. D* 55 (1997) 5613; J. Bijnens, G. Colangelo, P. Talavera, *JHEP* 9805 (1998) 014.

[26] J. Adams et al. [STAR Collaboration], *Phys. Rev. Lett.* 92 (2004) 092301.

[27] R. D. Pisarski, *Phys. Rev. D* 52 (1995), R3773.

[28] S. Pratt and W. Bauer, [arxiv:nucl-th/0308087](https://arxiv.org/abs/nucl-th/0308087).